

COVER PAGE

PAPER TITLE: A Curved, Elastostatic Boundary Element for Plane Anisotropic Structures

AUTHORS: Stanley S. Smeltzer III, NASA Langley Research Center, Eric C. Klang, North Carolina State University

ABSTRACT

The plane-stress equations of linear elasticity are used in conjunction with those of the boundary element method to develop a novel curved, quadratic boundary element applicable to structures composed of anisotropic materials in a state of plane stress or plane strain. The curved boundary element is developed to solve two-dimensional, elastostatic problems of arbitrary shape, connectivity, and material type. As a result of the anisotropy, complex variables are employed in the fundamental solution derivations for a concentrated unit-magnitude force in an infinite elastic anisotropic medium. Once known, the fundamental solutions are evaluated numerically by using the known displacement and traction boundary values in an integral formulation with Gaussian quadrature. All the integral equations of the boundary element method are evaluated using one of two methods: either regular Gaussian quadrature or a combination of regular and logarithmic Gaussian quadrature. The regular Gaussian quadrature is used to evaluate most of the integrals along the boundary, and the combined scheme is employed for integrals that are singular. Individual element contributions are assembled into the global matrices of the standard boundary element method, manipulated to form a system of linear equations, and the resulting system is solved. The interior displacements and stresses are found through a separate set of auxiliary equations that are derived using an Airy-type stress function in terms of complex variables. The capabilities and accuracy of this method are demonstrated for a laminated-composite plate with a central, elliptical cutout that is subjected to uniform tension along one of the straight edges of the plate. Comparison of the boundary element results for this problem with corresponding results from an analytical model show a difference of less than 1%.

Stanley S. Smeltzer III, Mechanics and Durability Branch, 8 W. Taylor St., NASA Langley Research Center, Hampton, VA 23681-2199.

Eric C. Klang, Mechanical and Aerospace Engineering Department, Box 7910, Raleigh, NC 27695-7910.

INTRODUCTION

Composite materials continue to see increased usage in space, aircraft, industrial, and recreational markets around the world. This upward trend is reflected in the recent advancements made for finite element methods; however, relatively few advances for boundary element methods (BEM) have been made for composite structures [1,2]. Boundary element advancements for composite structures are important, since boundary elements offer increased efficiency and accuracy over finite elements for infinite and semi-infinite regions, regions with large response gradients, and boundaries with complex geometry as well as reduced pre-processing time for discretizing a problem.

The initial application of the BEM to bodies composed of anisotropic materials was made by Rizzo [3]. Cruse presented a further advancement of the BEM in 1971 that included a derivation of the traction and displacement fundamental solutions for an anisotropic plate as well as determining stress concentrations for anisotropic plates with circular and elliptical cutouts [4]. Recent texts written about the BEM have focused on basic problems associated with isotropic structures as well as advanced topics in the areas of fracture mechanics [5], acoustics, and the evaluation of complex integrals for body forces and three-dimensional volumes [6].

The primary contribution of the curved, quadratic boundary element developed in the present paper is to provide a capability for modeling anisotropic regions that have highly curved boundaries. Instead of modeling a circular or elliptical boundary by using many straight elements to approximate the geometry, a relatively few curved elements can be used to model the geometry exactly with no loss in solution accuracy. An important aspect of the curved, quadratic boundary element resulting from the material anisotropy is the treatment of complicated singular integrals. The integrand of the singular integrals is an elaborate expression in terms of complex variables that results from the anisotropic material behavior, quadratic shape functions, and Gaussian quadrature evaluation points. All integrals are evaluated using the quadratic shape functions and Gaussian quadrature, which provides very accurate modeling of curvilinear boundaries. Thus, by careful manipulation of the singular integrals a sophisticated scheme has been developed for analyzing structures that are composed of anisotropic materials, have complex curved boundaries, and are in a state of plane strain or plane stress.

The objective of the present paper is to demonstrate a numerical method for evaluating elaborate, complex singular integrals that are used in the development of a curved, quadratic boundary element for structures composed of anisotropic materials that are in a state of plane stress or plane strain (referred to herein as plane anisotropic structures). This objective is accomplished by presenting the basic equations that govern a two-dimensional, linear elastostatic problem, the development of the boundary integral equation, the boundary element solution process, and the treatment of singular integrals using the developed method. A brief description of the modeling characteristics and analysis results for a classic structural mechanics problem is then presented to demonstrate the accuracy and computational efficiency of the curved boundary element for use with complex geometry.

THEORY

Boundary Integral Equation (BIE) Formulation

First, the equations that govern two-dimensional linear elastostatics as given by Brebbia are stated [7]. The equations of equilibrium are written using indicial notation as,

$$\sigma_{kl,l} + b_l = 0 \quad (k,l = 1,2) \quad \text{in } \Omega \quad (1)$$

where σ_{kl} are the components of the stress tensor, b_l are the components of the body-force vector, and Ω is the problem domain enclosed by a boundary denoted by Γ . The equations derived in this paper follow the rules of indicial notation; specifically, partial differentiation is represented by terms containing a comma and repeated indices indicate terms that are summed. The kinematic relations are

$$\varepsilon_{ij} = \frac{1}{2}(u_{i,j} + u_{j,i}) \quad (i, j = 1,2) \quad (2)$$

where ε_{ij} are the components of the strain tensor and u_i represents the components of the displacement vector. An additional equation that the strain components must satisfy when the displacement field is not the primary dependent variable is the compatibility equation. This equation in two dimensions is stated as

$$\varepsilon_{11,22} + \varepsilon_{22,11} = 2\varepsilon_{12,12} \quad (3)$$

Eq. 3 provides a necessary and sufficient condition for specified strain components to give displacements that are single-valued and continuous for simply connected regions. Since the problems of interest in the present paper are two-dimensional in nature, the constitutive equation for a state of plane stress is given for a plane anisotropic structure as

$$\begin{Bmatrix} \varepsilon_{11} \\ \varepsilon_{22} \\ 2\varepsilon_{12} \end{Bmatrix} = \begin{bmatrix} S_{11} & S_{12} & S_{16} \\ S_{12} & S_{22} & S_{26} \\ S_{16} & S_{26} & S_{66} \end{bmatrix} \cdot \begin{Bmatrix} \sigma_{11} \\ \sigma_{22} \\ \sigma_{12} \end{Bmatrix} \quad (4)$$

and

$$\varepsilon_{33} = S_{13}\sigma_{11} + S_{23}\sigma_{22} + S_{36}\sigma_{12} \quad (5)$$

where S_{ij} are the elements of the compliance matrix. In addition to eqs. 1-5, a set of boundary conditions is required to provide a complete description of the problem. The natural and essential boundary conditions are defined along the boundary Γ shown in Fig. 1 that consists of two distinct regions, Γ_1 and Γ_2 . The tick marks along the boundary in Fig. 1 represent the separation between the two boundaries. On Γ_1 , displacements are prescribed by

$$\bar{u}_i = u_i \quad (\text{on } \Gamma_1) \quad (6)$$

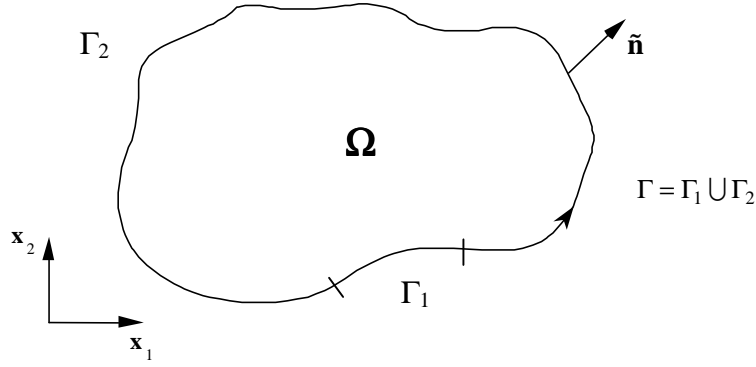


Figure 1: A general domain Ω with natural boundary conditions on Γ_2 and essential boundary conditions on Γ_1 .

and on Γ_2 , the tractions are prescribed by

$$\bar{p}_k = \sigma_{kj} \tilde{n}_j \quad (\text{on } \Gamma_2) \quad (7)$$

where \tilde{n}_j represents the components of the unit vector that is normal to Γ and that lies in the plane of the region Ω acted on by the traction.

The boundary value problem is reduced to a single partial differential equation by expressing the stresses in eq. 4 in terms of the Airy stress function and then substituting the strains in eq. 4 into the compatibility equation, eq. 2. The general solution of the resulting partial differential equation is obtained by following Lekhnitskii's method that uses a complex variable z given by $z = x + \mu y$, where μ is generally a complex number. Using this approach yields the following equation, known as the characteristic equation, which determines the values of μ :

$$S_{11}\mu^4 - 2S_{16}\mu^3 + (2S_{12} + S_{66})\mu^2 - 2S_{26}\mu + S_{22} = 0. \quad (8)$$

Lekhnitskii has shown that the four roots of eq. 8 are distinct and always imaginary as long as the material is not isotropic [8]. These roots can be denoted as,

$$\mu_k = \alpha_k + i\beta_k \quad \bar{\mu}_k = \alpha_k - i\beta_k \quad (k = 1, 2) \quad (9)$$

where the lowercase letter i denotes $\sqrt{-1}$. Once the values for μ are determined, the Airy stress function is expressed as a linear combination of complex potential functions. The forms of the complex potential functions are determined by the boundary conditions of a given problem.

A wide variety of analytical and numerical techniques may be employed to solve problems of the type described above. The technique used here involves numerical integration of the boundary integral equation (BIE) that is derived below. Specifically, the BIE is used to relate known displacement and traction values on the boundary to unknown values of interest within the domain. A convenient point to begin the derivation of the BIE was developed by Cruse and others by using

Somigliana's identity which relates the value of the displacements at any point in Ω to the boundary values [9], u_j and p_j , such that

$$u_i(\xi) = \int_{\Gamma} u_{ij}^*(\xi, x) p_j(x) d\Gamma(x) - \int_{\Gamma} p_{ij}^*(\xi, x) u_j(x) d\Gamma(x) \quad (10)$$

where p_j is defined by the right hand side of eq. 7 and ξ and x are functions of x_1 and x_2 . The values u_{ij}^* and p_{ij}^* represent fundamental solutions that describe the displacements and tractions, respectively, in the j direction at point x corresponding to a unit-magnitude point force acting in the i direction of an infinite material applied at point ξ . The foundation for eq. 10 is the use of an arbitrary complimentary load case, represented by the terms with an asterisk. In this development, the load case is defined as a point force acting over an infinitesimally small area at a position ξ referred to as a "source point." A mathematical function used to describe the point force is the Dirac delta function described by Paris [6]. Since the problems of interest in this study have anisotropic material properties, the fundamental solutions for an anisotropic medium are used to develop the required boundary element equations. The fundamental solutions for an anisotropic body were determined by Cruse using a complex Airy stress function and are reproduced below [4]:

$$u_{ji}^* = 2 \cdot \Re \left\{ P_{i1} A_{j1} \log[z_1(\xi, x)] + P_{i2} A_{j2} \log[z_2(\xi, x)] \right\} \quad (11)$$

$$\begin{aligned} \text{where } P_{jk} &= S_{11}\mu_k^2 + S_{12} - S_{16}\mu_k \quad (i, j, k = 1, 2) \\ P_{2k} &= S_{12}\mu_k + \frac{S_{22}}{\mu_k} - S_{26} \quad (i, j, k = 1, 2) \end{aligned}$$

and

$$p_{ji}^* = 2 \cdot \Re \left\{ Q_{i1} (\mu_1 \tilde{n}_1 - \tilde{n}_2) \frac{A_{j1}}{z_1(\xi, x)} + P_{i2} A_{j2} \log[z_2(\xi, x)] \right\} \quad (12)$$

$$\text{where } [Q_{ik}] = \begin{bmatrix} \mu_1 & \mu_2 \\ -1 & -1 \end{bmatrix} \quad (i, j, k = 1, 2)$$

and the A_{ji} values are obtained from the solution of a 4x4 matrix of equations that are not presented here because of their excessive length, but may be found in [4].

The choice for the location of the evaluation point ξ given in eq. 10 is arbitrary; however, it is necessary to evaluate all the terms along the boundary Γ to form the BIE. A consequence of evaluating the arbitrary point ξ along the boundary is that singularities will occur at certain points within the fundamental solutions given by eqs. 11 and 12. These special cases of singular boundary points are referred to as coincident source and field points. As the distance between the source and field points shrinks to zero, the singularity occurs during the numerical integration of these boundary integrals. Therefore, the following equation results from the evaluation of eq. 10 along the boundary and is the integral form of the BIE

$$c_{ij}(\xi)u_j(\xi) + \int_{\Gamma} p_{ij}^*(\xi, x)u_j(x) \cdot d\Gamma = \int_{\Gamma} u_{ij}^*(\xi, x)p_j(x) \cdot d\Gamma \quad (13)$$

where c_{ij} constitutes a 2x2-coefficient matrix for u_j that occurs because of a singularity on the boundary and i and j can have the values of one or two. The precise values of c_{ij} are determined by evaluating the boundary integrals in eq. 13 by using Cauchy principal values that are dependent on the local boundary geometry in the neighborhood of the point under evaluation. However, explicit evaluation of the terms in the c_{ij} matrix is not necessary since it was shown by Brebbia that the effects of a unit rigid-body displacement might indirectly calculate them [7]. Equation 13 may also be written using matrix notation as,

$$\mathbf{C}\mathbf{u} + \int_{\Gamma} \mathbf{P}^* \mathbf{u} \cdot d\Gamma = \int_{\Gamma} \mathbf{U}^* \mathbf{p} \cdot d\Gamma \quad (14)$$

Using eq. 14 and the boundary conditions from eqs. 6 and 7, the unknown displacements and tractions on the boundary are determined.

Interior Displacements, Strains, and Stresses

The interior (boundary excluded) displacements, strains, and stresses are all determined by using Somigliana's identity once the unknown boundary values have been determined. The interior displacements are calculated directly from eq. 10, while the strains and stresses require additional attention. Differentiating eq. 10, the strain tensor is obtained using the kinematic relation of eq. 2

$$2\varepsilon_{jl} = \int_{\Gamma} \left[\frac{\partial p_{ji}^*}{\partial x_l} + \frac{\partial p_{li}^*}{\partial x_j} \right] u_i \cdot d\Gamma - \int_{\Gamma} \left[\frac{\partial u_{ji}^*}{\partial x_l} + \frac{\partial u_{li}^*}{\partial x_j} \right] p_i \cdot d\Gamma \quad (15)$$

or

$$2\varepsilon_{jl} = \int_{\Gamma} S_{jli} u_i \cdot d\Gamma - \int_{\Gamma} D_{jli} p_i \cdot d\Gamma \quad (16)$$

where the derivatives of the fundamental solutions in eq. (15) have been evaluated by Cruse [4] and are reproduced below as

$$S_{jli} = -2 \cdot \Re e \left\{ R_{l1} Q_{i1} (\mu_1 \tilde{n}_1 - \tilde{n}_2) \frac{A_{j1}}{z_1^2} + R_{l2} Q_{i2} (\mu_2 \tilde{n}_1 - \tilde{n}_2) \frac{A_{j2}}{z_2^2} \right\} \\ - 2 \cdot \Re e \left\{ R_{j1} Q_{i1} (\mu_1 \tilde{n}_1 - \tilde{n}_2) \frac{A_{l1}}{z_1^2} + R_{j2} Q_{i2} (\mu_2 \tilde{n}_1 - \tilde{n}_2) \frac{A_{l2}}{z_2^2} \right\} \quad (17)$$

and

$$D_{jli} = 2 \cdot \Re e \left\{ \frac{R_{l1} P_{i1} A_{j1}}{z_1} + \frac{R_{l2} P_{i2} A_{j2}}{z_2} \right\} \\ + 2 \cdot \Re e \left\{ \frac{R_{j1} P_{i1} A_{l1}}{z_1} + \frac{R_{j2} P_{i2} A_{l2}}{z_2} \right\} \quad (18)$$

where the indices i, j , and l can have values equal to one or two, P_{ij} and Q_{ij} are as defined in eqs. 11 and 12, and $R_{lk} = 1$ and $R_{2k} = \mu_k$ for $k = 1, 2$. Thus, the interior strains are obtained directly from eqs. 16-18. The interior stresses are then determined by substituting the calculated strains into the constitutive relationship given by eq. 4.

Solution Procedure

The standard BEM solves complex problems by discretizing the boundary into elements and nodes, and this approach allows piecewise solution of a BIE like that given in eq. 14. To allow a better numerical treatment of a BIE that accurately represents curved boundaries, eq. 14 is rewritten in a discretized element format as

$$c_k u_k + \sum_{k=1}^N \hat{H}_{lk} u_k = \sum_{k=1}^N G_{lk} p_k \quad (19)$$

where u_k and p_k are the displacements and tractions, respectively, for node “ k ” and N is the total number of nodes for the problem. The variable l represents the arbitrary source point and the \hat{H} and G matrices are written as

$$\hat{H}_{lk} = \sum_{L=1}^{NEL} \int_{\Gamma_L} p^* \phi d\Gamma \quad (20)$$

and

$$G_{lk} = \sum_{L=1}^{NEL} \int_{\Gamma_L} u^* \phi d\Gamma \quad (21)$$

where NEL represents the total number of elements comprising the discretized region, Γ_L is the boundary curvature of the L^{th} element, and ϕ is an array containing the assumed shape functions. Since u_k in eq. 19 contain unknown displacements, eq. 19 is simplified by combining the c_k and \hat{H}_{lk} matrices for the two unknown displacement vectors in the following manner,

$$\begin{aligned} \text{when } l = k, & \quad H_{lk} = \hat{H}_{lk} + c_k \text{ and} \\ \text{when } l \neq k, & \quad H_{lk} = \hat{H}_{lk}. \end{aligned}$$

Simplifying eq. 19,

$$\sum_{k=1}^N H_{lk} u_k = \sum_{k=1}^N G_{lk} p_k \quad (22)$$

or in matrix form

$$\mathbf{H} \mathbf{u} = \mathbf{G} \mathbf{p} \quad (23)$$

which represents all the contributions by the source point I into a global system of equations. Equation 23 will produce a system of equations in which known and unknown values are scattered between the two vectors, \mathbf{u} and \mathbf{p} . The known and unknown values are redistributed in a manner that places all known values in one vector and all unknown values in the other vector, which yields a desirable system of equations in the standard form $\mathbf{Ax}=\mathbf{b}$.

Singular Integrals

The method presented in this paper involves numerical integration of the boundary integral equation as opposed to exact solution of the individual terms in eqs. 20 and 21. All the integrals containing non-singular functions in this paper are evaluated using the 8-point, regular form of Gaussian quadrature given by

$$I = \int_{-1}^{+1} f(x)dx \cong \sum_{i=1}^n w_i f(\xi_i) \quad (24)$$

where w_i are the weighting functions and ξ_i are the integration points. In the cases where the integrand has a logarithmic singularity, it is necessary to manipulate the integrand to obtain a form that may be evaluated using the logarithmic Gaussian quadrature or a combination of the regular and the logarithmic Gaussian quadrature forms. The logarithmic Gaussian quadrature form is written as,

$$I = \int_0^1 \ln\left(\frac{1}{x}\right) f(x)dx \cong \sum_{i=1}^n w_i f(\xi_i) \quad (25)$$

where the weighting function w_i and the integration point ξ_i are not the same as those for the regular Gaussian quadrature.

An important aspect of the BEM development is the relationship between an arbitrary boundary element and a general source point. The orientation of the boundary element, its distance from the source point, and the locations of the nodal positions are illustrated in Figure 2a. The element represented in Figure 2 is

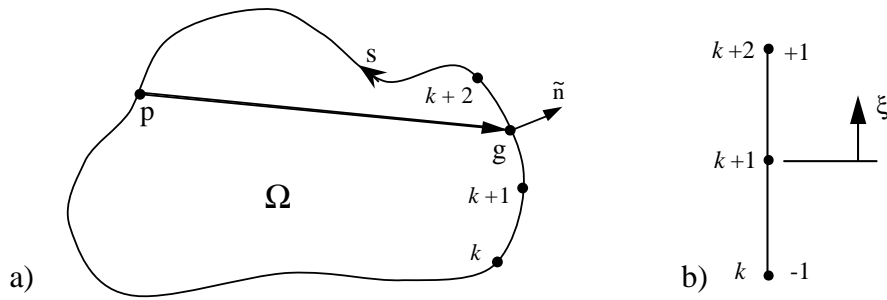


Figure 2: Actual and mapped coordinate systems for an element;
a) original (actual) element and b) mapped element.

quadratic and is used to describe both the geometry and displacement values for this method. The element shown in Figure 2b represents the mapping of the originally curved, quadratic element into a transformed coordinate system. Initially, a description of the x and y coordinate of any point along an element is given by its nodal coordinates in conjunction with the corresponding shape functions, i.e.,

$$x = \phi_1 x_k + \phi_2 x_{k+1} + \phi_3 x_{k+2} \quad (26)$$

$$y = \phi_1 y_k + \phi_2 y_{k+1} + \phi_3 y_{k+2} \quad (27)$$

where

$$\phi_1 = -\frac{1}{2}\xi(1-\xi) \quad (28)$$

$$\phi_2 = 1-\xi^2 \quad (29)$$

$$\phi_3 = \frac{1}{2}\xi(1+\xi) \quad (30)$$

The distance from the source point p to a field point g on the boundary is the square root of the square of the x and y distances between the points. However, for an anisotropic material, the incorporation of complex variables into the solution requires that the description of the distance to a field point on the boundary take the following form

$$z_k = (x_g - x_p) + \mu_k (y_g - y_p) \quad (31)$$

where μ_k are the roots of the characteristic equation defined by eq. 8.

The singularities of the BIE are determined by finding the locations where the source and field points are coincident in the \mathbf{H} and \mathbf{G} matrices defined by eq. 23. cursory examination of the \mathbf{H} and \mathbf{G} matrices reveals that the contributions from the source point, i.e. the singular terms, only occur along the diagonal of each matrix. The location of these singular terms along the diagonals is an important characteristic that will allow the singularities of the \mathbf{H} matrix in eq. 20 to be dealt with directly. First, recall from the section on formulating the BIE that the diagonal of the \mathbf{H} matrix was determined by combining the c_i and H_{ii} terms because of the effects of a unit rigid-body displacement on the domain Ω . In particular, the right hand side of eq. 22 must equal zero for a unit rigid-body displacement, which allows the diagonal elements of the \mathbf{H} matrix to be expressed in terms of the off-diagonal elements of the \mathbf{H} matrix. Therefore, the explicit evaluation of all the singular terms in the \mathbf{H} matrix has been avoided by assuming a unit rigid-body displacement. The \mathbf{G} matrix, in contrast, requires direct evaluation of each singular integral along its diagonal. The elements of the \mathbf{G} matrix are comprised of the shape-function matrix ϕ and the fundamental solution u^* . The shape-function matrix is simply a function of the Gaussian coordinate ξ and, consequently, contains no singularities. Therefore, the only function that contains a singularity is the fundamental solution for the displacements given by eq. 11. In order to deal with the singularities in the \mathbf{G} matrix, the functions must be manipulated to allow Gaussian integration of each element. In addition, three special cases of coincident source and field points exist which produce a singularity. An example for each of

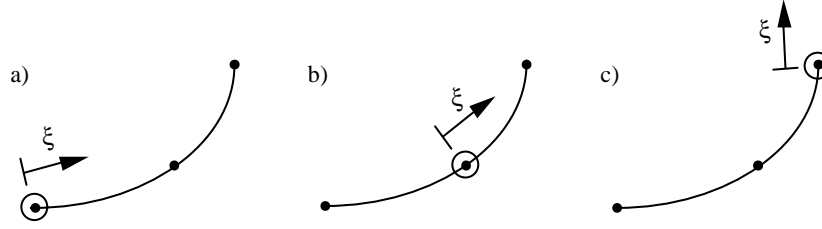


Figure 3: A general boundary element and the three special cases of coincident source and field points; a) $l=k$, b) $l=k+1$, and c) $l=k+2$.

these cases is illustrated in Figure 3 where the source point ξ coincides with some field point k ; such that $l=k$, $l=k+1$, or $l=k+2$.

The singular integrands of the \mathbf{G} matrix must be rewritten to deal with the singularity at the coincident source and field points. The values of the natural logarithm function of the complex variables z_1 and z_2 in eq. 11 are the only terms that are not a constant, and thus contain the terms that become singular. The first step towards managing the singular functions of the \mathbf{G} matrix involves rewriting the expression for the distance between the source and the field points. By expanding the complex variable z_k , a more convenient form of the variable is obtained that both fits Gaussian quadrature and allows isolation of the singularity. This change of format is shown in eq. 31 as the distance from the source point to the field point in terms of rectangular coordinates is more conveniently written using polar coordinates as

$$\ln(z_k) = \ln(r_k e^{i\theta_k}) \quad (32)$$

where

$$r_k = \sqrt{(x_d + \alpha_k y_d)^2 + (\beta_k y_d)^2},$$

$$\theta_k = \tan^{-1}\left(\frac{\beta_k y_d}{x_d + \alpha_k y_d}\right),$$

$$x_d = (x_g - x_p), \text{ and}$$

$$y_d = (y_g - y_p).$$

Now, consider the case when the source and the field points are coincident ($l=k$, in Figure 3a). The singular integral is of the form

$$\int_0^s \ln(re^{i\theta}) \phi_j \cdot dS \quad j = 1, 2, 3. \quad (33)$$

Separating the kernel of eq. 33, rewriting the integrals in Gaussian integration format, and setting them equal to an arbitrary value I_1 for convenience, such that

$$I_1 = \int_{-1}^{+1} \ln[r(\xi)] \phi_j(\xi) \det[\mathbf{J}] \cdot d\xi + \int_{-1}^{+1} i\theta(\xi) \phi_j(\xi) \det[\mathbf{J}] \cdot d\xi \quad (34)$$

which can be rewritten as $I_1 = I_2 + I_3$. The second integral, I_3 , is nonsingular since it approaches zero as the radius goes to zero, so I_3 in equation 34 can be evaluated by simply using regular Gaussian quadrature. In order to evaluate the first integral, I_2 , a change of limits is required because of the singularity. First, the limits of I_2 are changed to 0 to 1 (from -1 to +1)

$$I_2 = \int_0^1 \ln[r(\eta)] \phi_I(\eta) \det[\mathbf{J}] \cdot 2 \cdot d\eta \quad (35)$$

and then the numerator and denominator of the kernel are multiplied by η and separated as shown below

$$I_2 = \int_0^1 \ln \left[\frac{r(\eta)}{\eta} \right] \cdot \phi_I(\eta) \cdot \det[\mathbf{J}] \cdot 2 \cdot d\eta - \int_0^1 \ln \left[\frac{1}{\eta} \right] \cdot \phi_I(\eta) \cdot \det[\mathbf{J}] \cdot 2 \cdot d\eta \quad (36)$$

which can again be rewritten as $I_2 = I_4 + I_5$. Thus, the problem of the singularity has been resolved in I_2 by splitting the integral into two integrals that are more manageable. The first integral I_4 can be shown to be non-singular using L'Hopital's rule which enables it to be integrated using the regular Gaussian quadrature. The second integral, I_5 , has been conveniently manipulated into the logarithmic Gaussian quadrature format, such that

$$I_5 = \int_0^1 \ln \left[\frac{1}{\eta} \right] \phi_I(\eta) \det[\mathbf{J}] \cdot 2 \cdot d\eta \cong \sum_{k=1}^N [\phi_I(\eta_k) \det[\mathbf{J}] \cdot 2]_k w_k \quad (37)$$

Returning to I_4 , the limits of integration need to be adjusted to facilitate the use of regular Gaussian quadrature, so

$$I_4 = \int_{-1}^{+1} \ln \left[\frac{r(\xi)}{\left(\frac{\xi+1}{2} \right)} \right] \phi_I(\xi) \det[\mathbf{J}] \cdot d\xi \quad (38)$$

Finally, for the case of coincident source and field point, when $l=k$, we can write the integral I_1 as,

$$\int_0^s \ln(re^{i\theta}) \phi_j \cdot dS \cong \sum_{m=1}^{N_{rg}} \left\{ \ln \left[\frac{r(\xi_m)}{\left(\frac{\xi_m+1}{2} \right)} \right] + i\theta(\xi_m) \right\} \cdot \phi_j(\xi_m) \cdot \det[\mathbf{J}] \cdot w_{rg} - \sum_{n=1}^{N_{lg}} \phi_j(\eta_n) \cdot \det[\mathbf{J}] \cdot 2 \cdot w_{lg} \quad (39)$$

where N_{rg} are evaluation points used for the regular form of Gaussian quadrature and N_{lg} are evaluation points used for the logarithmic form of Gaussian quadrature. Equation 39 does not contain any singularities and may be evaluated at any point under consideration. Also, note that a sequence of coordinate mappings was used to determine eq. 39. Therefore, it is very important to remember the critical information; the radius $r(\xi)$, the shape function ϕ_j , and the Jacobian \mathbf{J} must always be calculated in terms of the original coordinate ξ . The process of removing singularities for the other two cases of coincident source and field points, when $l=k+1$ and $l=k+2$, are very similar to the previous derivation and the complete derivations are available in earlier work by Smeltzer [10].

NUMERICAL RESULTS

The BEM presented in the previous section was evaluated by using a quasi-isotropic plate with an elliptical cutout. The quasi-isotropic plate configuration discussed in the present paper was chosen for convenience, and essentially demonstrates the full capabilities of the curved, quadratic boundary element. The plate under consideration is square with an edge length of 10 inches and was loaded by subjecting two of the straight edges of the plate to uniform tension in the direction of the x_1 -axis. The elliptical cutout is at the center of the plate and has a major axis of 0.1 inches and a minor axis of 0.05 inches where the minor axis is aligned with the x_1 -axis. A half-plate model of the plate with the appropriate symmetry conditions was used with 54 quadratic boundary elements, and only eight of those elements were used to model the boundary of the elliptical cutout. The effective, laminate material properties for the $[0, \pm 45]_s$ plate are given in Table 1. In addition, the subscripts 1 and 2 for the material properties given in Table 1 refer to the coordinate directions of the structure and not the principal material coordinate directions of a laminate ply.

The analytical solution for an infinite plate is given by Lekhnitskii and is plotted in Figure 4 along with the BEM solution [8]. Correlation between the analytical solution and the corresponding BEM solution is excellent, with an error of less than 1%. In addition, the figure shows a stress concentration at the edge of the elliptical cutout equal to 3.74 times the far-field traction P .

TABLE 1: BASIC MATERIAL PROPERTIES FOR THE COMPOSITE PLATE

Laminate	Roots of Characteristic Equation (8)	Effective, Laminate Material Properties
$[0, \pm 45]_s$	$\mu_1 = 0.7921 + 0.9659i$ $\mu_2 = -0.7921 + 0.9659i$	$E_1 = 7.706 \times 10^6$ psi $E_2 = 3.164 \times 10^6$ psi $\nu_{12} = 0.794$ $G_{12} = 3.504 \times 10^6$ psi

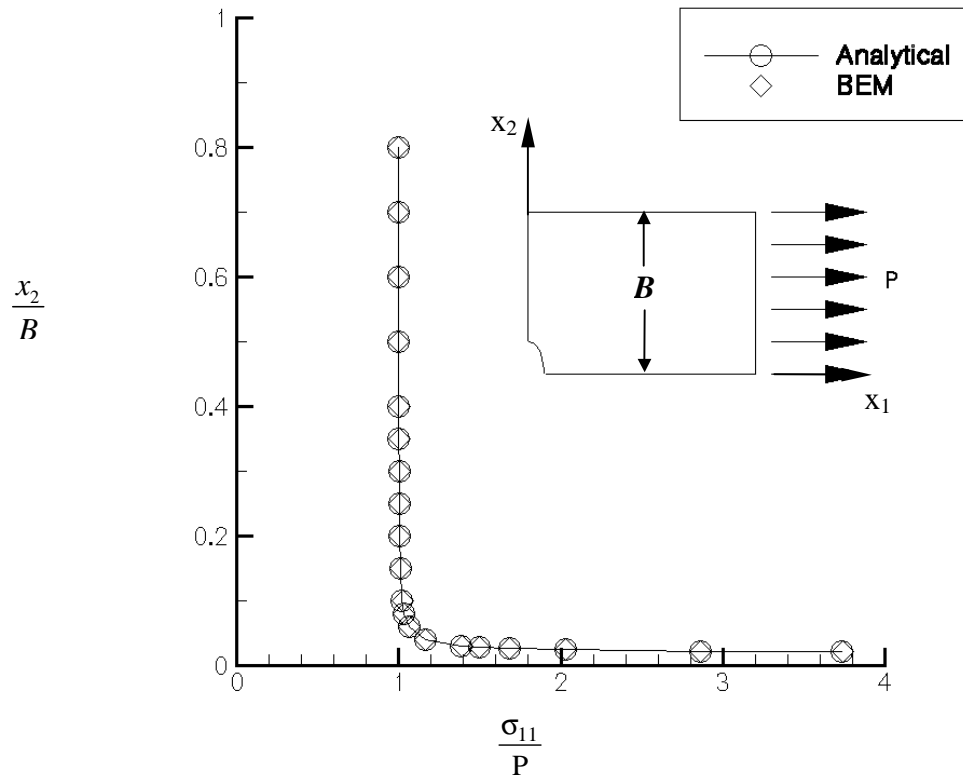


Figure 4: The stress distribution along the positive x_2 -axis for a $[0,\pm 45]_s$ composite laminate with an elliptical cutout.

CONCLUDING REMARKS

A method has been presented in the present paper that details the development of a novel, curved, quadratic boundary element for analyzing structures composed of anisotropic materials in a state of plane stress or plane strain. Although the standard boundary element method (BEM) equations for elastostatics were employed in the development of the curved boundary element, elaborate singular integrals were derived because of the nature of the complex fundamental solutions for an anisotropic material. The treatment of these singular integrals was a key component of the boundary element derivation presented herein, and was complicated further by allowing the boundary element to be curved. The complexity of the singular integrals was handled by performing a sequence of coordinate mappings on the curved elements that resulted in an expression that was amenable to Gaussian quadrature. Thus, the curved elements were mapped to a new coordinate system that facilitated removal of the singularities and allowed for accurate and efficient

evaluation of the integrals. The basic framework and solution technique for the curved BEM was illustrated and a comparison of the results for a curved, quadratic boundary element with those for a classic problem in engineering mechanics showed differences of less than 1%.

1. Deb, A., Henry, D.P., and Wilson, R.B., "Alternative boundary element method formulations for 2- and 3-D anisotropic thermoelasticity," *Int. J. of Solids and Struc.*, **27**-13, pp. 1721-1738, 1991.
2. Schlar, N.A., *Anisotropic Analysis Using Boundary Elements*, Computational Mechanics Publications, Boston, 1994.
3. Rizzo, F.J. and Shippy, D.J., "A method for stress determination in plane anisotropic elastic bodies," *J. Comp. Matls.*, **4**, pp. 36-61, 1970.
4. Cruse, T.A. & Swedlow, J.L., "Interactive program for analysis and design problems in advanced composite technology", AFML-TR-71-268, pp. 160-273, 1971.
5. Trevelyan, J., *Boundary Elements for Engineers – Theory and Application*, Computational Mechanics Publications, Boston, 1994.
6. Paris, F. & Canas, J., *Boundary Element Method*, Oxford University Press, New York, pp. 4-7, 1997.
7. Brebbia, C.A., Telles, J.C.F. and Wrobel, L.C., *Boundary Element Techniques: Theory and Applications in Engineering*, Springer-Verlag, pp. 199-202, London, 1984.
8. Lekhnitskii, S.G., *Theory of Elasticity of an Anisotropic Elastic Body*, Mir Publishers, Moscow, 1981.
9. Cruse, T.A., "An improved boundary-integral equation method for three dimensional elastic stress analysis", *Comput. and Struct.*, **4**, pp. 741-754, 1974.
10. Smeltzer III, S.S., "A two dimensional boundary element method for generally anisotropic materials," M.S. Thesis, North Carolina State University, 1991.